Regulated Pole-to-Pole Oscillations of a Bacterial Gliding Motility Protein

Tâm Mignot *et al.*

Science **310**, 855 (2005);
DOI: 10.1126/science.1119052

31. D. S. Aaronson, C. M. Horvath, *Science* **296**, 1653 (2002).
32. Treatment with 3,4-DAA was associated with a markedly suppressed lymphocytic infiltration in the spinal cords of mice with EAE (fig. S4).
33. I. L. Tan, G. J. Lycklama a Nijeholt, C. H. Polman, H. J. Ader, F. Barkhof, *Mult. Scler.* **6**, 99 (2000).
34. C. Polman *et al.*, *Neurology* **64**, 987 (2005).
35. This work was supported by grants from the NIH, the National MS Society, the Phil N. Allen Trust to L.S., and funding from Angiogen Pharmaceuticals Pty. Ltd. M.P. is a recipient of an Emmy-Noether-Fellowship from the German Research Foundation (Deutsche Forschungsgemeinschaft, DFG PL 315/1-1). M.S. is a major stockholder of Angiogen Pharmaceuticals Pty. Ltd., which develops and commercializes new therapies in inflammation, neurological disease, and cancer. We thank M. J. Eaton and M. Britschgi for excellent technical assistance. K. Yokoyama and H. McDevitt kindly provided the MBP Ac1-11 TCR transgenic mice used for the gene microarray studies.

Supporting Online Material
www.sciencemag.org/cgi/content/full/310/5749/850/DC1
Materials and Methods
Figs. S1 to S5
Tables S1 to S5
References and Notes

19 July 2005; accepted 5 October 2005
10.1126/science.1117634

Regulated Pole-to-Pole Oscillations of a Bacterial Gliding Motility Protein

Tâm Mignot, John P. Merlie Jr., David R. Zusman*

Little is known about directed motility of bacteria that move by type IV pilus–mediated (twitching) motility. Here, we found that during periodic cell reversals of *Myxoccocus xanthus*, type IV pili were disassembled at one pole and reassembled at the other pole. Accompanying these reversals, FrzS, a protein required for directed motility, moved in an oscillatory pattern between the cell poles. The frequency of the oscillations was controlled by the Frz chemosensory system, which is essential for directed motility. Pole-to-pole migration of FrzS appeared to involve movement along a filament running the length of the cell. FrzS dynamics may thus regulate cell polarity during directed motility.

Gliding motility is important for bacterial movement on solid surfaces, virulence, and development (*1*). Twitching motility in *Pseudomonas aeruginosa* or social motility (S-motility) in *Myxococcus xanthus* involves assembly of type IV pili at the leading end of cells: Motion is produced as the fibers bind to receptors on the substratum, or another cell, and retract (*2*). Control of directional movements requires periodic cell reversals, which are regulated by chemosensory systems (*1*, *3*, *4*). It has been proposed that cellular reversals are achieved by switching the sites of pili extrusion from one cell pole to the other (*4*).

In *M. xanthus*, directed motility allows cells to coordinate movements toward nutrients or, when limiting, fruiting bodies (*5*). FrzS is required for S-motility–dependent vegetative swarming. It contains an N terminal receiver–like domain, an alanine-proline–rich linker, and an extended coiled-coil domain (fig. S1A) (*6*). *frzS* mutants are impaired in S-motility swarming because they are defective in regulating pili–mediated directional movements (fig. S1, B and C). Indeed, mutants that have strong directional defects cannot swarm or form fruiting bodies (*7*, *8*).

University of California, Department of Molecular and Cell Biology, Berkeley, CA 94720–3204, USA.

*To whom correspondence should be addressed. E-mail: zusman@uclink.berkeley.edu

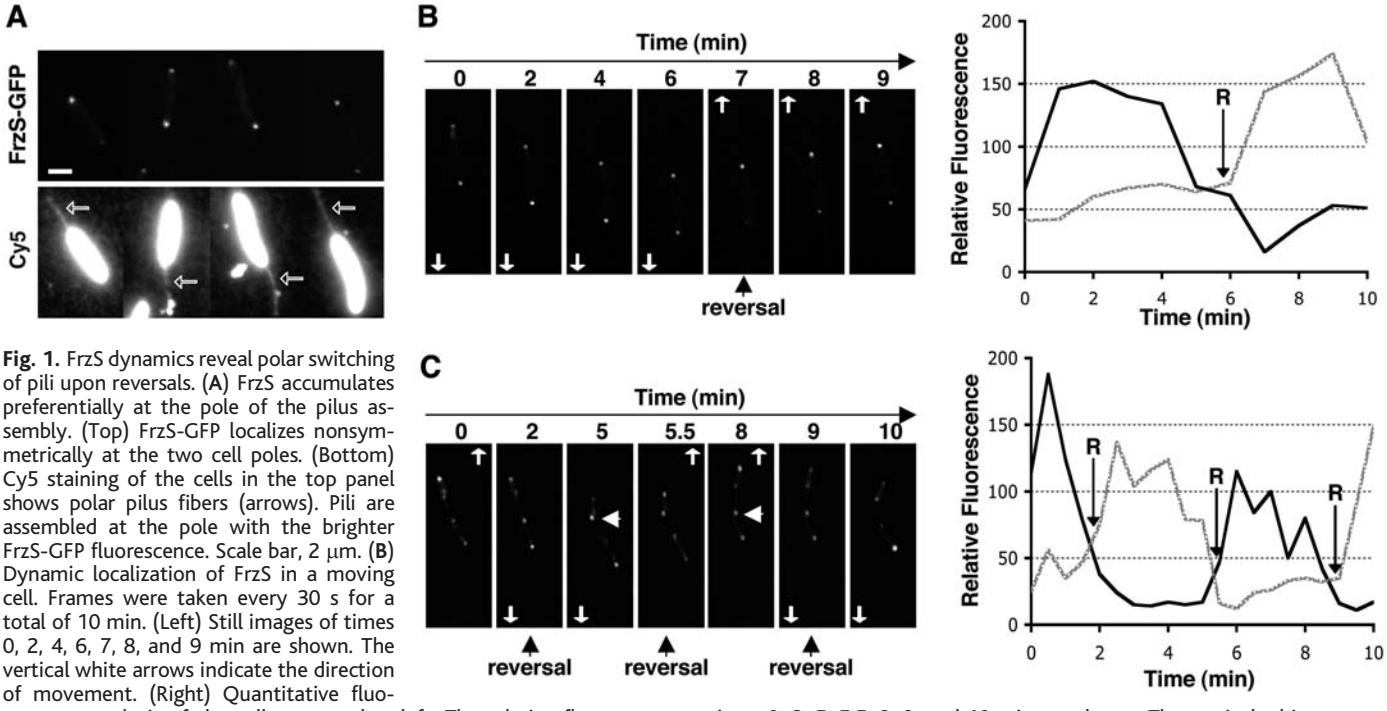

Fig. 1. FrzS dynamics reveal polar switching of pili upon reversals. (**A**) FrzS accumulates preferentially at the pole of the pilus assembly. (Top) FrzS-GFP localizes nonsymmetrically at the two cell poles. (Bottom) Cy5 staining of the cells in the top panel shows polar pilus fibers (arrows). Pili are assembled at the pole with the brighter FrzS-GFP fluorescence. Scale bar, 2 μm. (**B**) Dynamic localization of FrzS in a moving cell. Frames were taken every 30 s for a total of 10 min. (Left) Still images of times 0, 2, 4, 6, 7, 8, and 9 min are shown. The vertical white arrows indicate the direction of movement. (Right) Quantitative fluorescence analysis of the cell presented at left. The relative fluorescence intensities (arbitrary units) of each cell pole were measured and plotted over time. Black line, initial leading pole; gray line, initial trailing pole; R, Reversal. (**C**) Dynamic localization of FrzS in a *frzCD*^{c} mutant cell. Frames were taken every 30 s for a total duration of 10 min. (Left) Still images of times 0, 2, 5, 5.5, 8, 9, and 10 min are shown. The vertical white arrows indicate the direction of movement. Horizontal white arrows point to *frzCD*^{c} –dependent additional FrzS spots that brighten immediately before switch of the bright pole. (Right) Quantitative fluorescence analysis of the cell presented at left. Labels as in (B).

To investigate the cellular localization of FrzS, we constructed a strain containing green fluorescent protein (GFP) in a chimeric *frzS-gfp* gene in place of the endogenous *frzS* gene (fig. S2A). The FrzS-GFP fusion protein was stably expressed and functional (fig. S2, B and C). FrzS-GFP was localized in patches primarily at both cell poles (Fig. 1A). In many cells, one pole was bright and the other dim, which suggested that FrzS accumulated at one pole in preference to the other (Fig. 1A). The brighter FrzS-GFP pole usually corresponded to the pole containing pili (37 of 40 analyzed cells), visualized with Cy5 (Fig. 1A), a nonspecific fluorescent dye that has been used to label pilus fibers in *P. aeruginosa* (*9*). We followed individual cells expressing FrzS-GFP as they moved on agar pads by time-lapse fluorescence microscopy. As expected, the brighter FrzS-GFP fluorescent patch was typically observed at the leading end of the cell (Fig. 1B and Table 1).

Table 1. Correlation between FrzS localization pattern and cellular reversals. Total cells is the number of filmed cells for each strain. Bright leading poles were unambiguously asymmetrical with a brighter patch at the leading pole. Dim leading poles were unambiguously asymmetrical with a dimmer patch at the leading pole. No symmetry means cells displayed movement with no evident FrzS asymmetry. A reversal was scored each time a cell changed its direction by 180°. A switch was scored each time a brighter pole became a dimmer pole. Percent correlation reflects the percentage of cells where a switch occurred concurrently with a reversal.

Measure	Background		
	WT	*frzE*	*frzCD*^{c}
Total cells	92	94	34
Scored cells			
Bright leading pole	86	84	34
Dim leading pole	4	5	0
No asymmetry	2	5	0
Reversals	33	8	92
Switch	33	0	92
Percent correlation	100	0	100

If cellular reversals involve pole-to-pole switching of pili fibers, then we should see relocalization of the brighter FrzS-GFP fluorescent patch from one cell pole to the other when a cell reverses. As predicted, fluorescence at the leading pole slowly decreased and gradually increased at the trailing pole so that the intensity was equalized at both poles after 5 to 6 min (Fig. 1B; movie S1). Fluorescence at the leading pole then dispersed, and the cell reversed direction causing the old trailing pole to become both the brighter pole and the new leading pole. FrzS-GFP fluorescence increased rapidly at the new leading pole as the cell continued to move in the new direction (Fig. 1B). Thereafter, fluorescence at the leading pole decreased as the trailing pole showed increased fluorescence. We tracked 92 cells for 10-min intervals and observed 33 cells reversing; cell reversal was always accompanied by relocalization of the brighter fluorescent patch from the old leading cell pole to the new leading cell pole (Table 1). Thus, pili switched poles when cells reversed, and FrzS was associated with the regulation of the switch.

The Frz chemosensory pathway acts as a biochemical regulator of cell reversals (*10*). *frz* mutants very rarely reverse their direction of movement and are defective in swarming and fruiting body formation (*11*). We monitored FrzS-GFP oscillations in a *frz*-null mutant (*frzE*) to determine whether the Frz pathway modulates FrzS dynamics. Although most cells still had the brighter fluorescent patch at the leading cell pole, pole-to-pole oscillations of FrzS were not observed in this mutant (Table 1). Rarely, a cell was observed to reverse its direction of movement, but then FrzS polar switching failed to occur (Table 1). These reversal events may have been caused by unregulated activity of the other motility motor, the A-motility system (see fig. S1). Some *frz* mutants (*frzCD*^{c}) show hyperreversals, hypothesized to be caused by constitutive signaling through the Frz pathway (*11*). FrzS-GFP–expressing strains containing the *frzCD*^{c} mutation showed a ninefold increase in reversal frequency; these reversals were always accompanied by FrzS polar switching (Table 1). A fluorescence microscopy time-lapse series of a FrzS-GFP *frzCD*^{c} mutant cell is shown (Fig. 1C; movie S2). The cell pictured reversed its direction three times in the 10-min filming interval and showed corresponding oscillations in FrzS-GFP localization. The oscillatory period of FrzS-GFP was markedly reduced in the mutant, but the pattern was very similar to the one observed in the parent strain: Reversals always happened together with dispersal of the fluorescence at the old leading pole (after equalization of the fluorescent signals at both poles), followed by a rapid increase in fluorescence at the new leading pole. Additional nonpolarly localized FrzS clusters

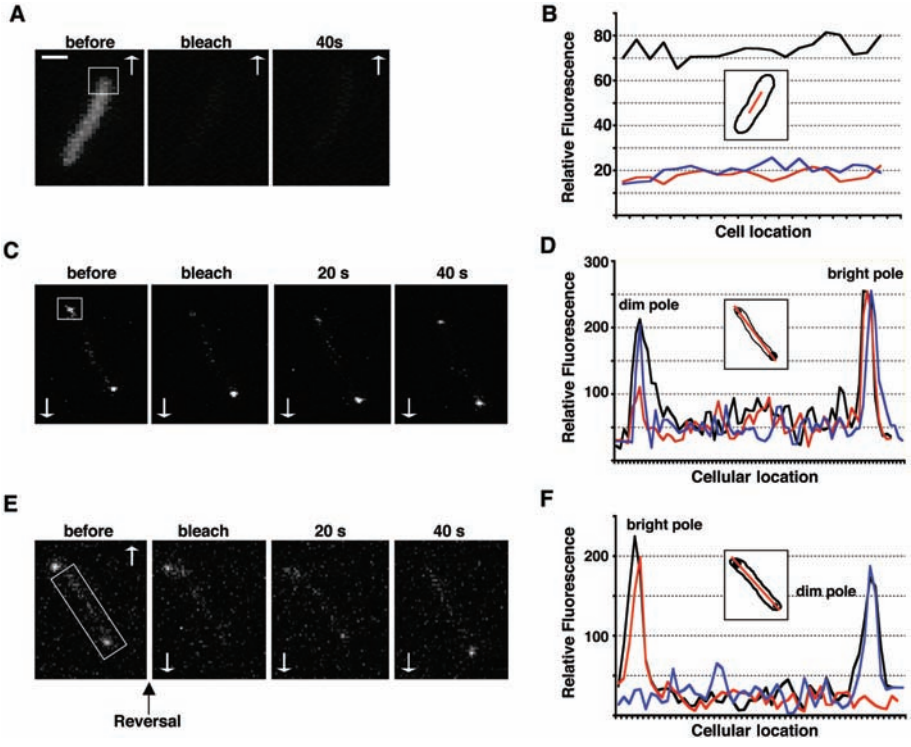

Fig. 2. FrzS-GFP dynamics in moving cells. (**A**) Diffusible GFP is fully bleached in the course of a 10-s laser exposure of the cell pole. Micrographs of a cell before bleaching, immediately after bleaching, and 40 s after bleaching. The open rectangle shows the area exposed to the laser. The white arrow shows the direction of movement. Scale bar, 2 μm. (**B**) Quantitative fluorescence analysis of the cell presented in (A) at different times. The relative fluorescence intensities (arbitrary units) were plotted as a function of the cellular location. Black line, fluorescence intensities before photobleaching; red line, fluorescence intensities immediately after photobleaching; blue line, fluorescence intensities 40 s after photobleaching. The inset represents the region of the cell that was selected (red line) to obtain the fluorescence intensity profile. (**C**) FRAP analysis of FrzS-GFP fluorescence at the dimmer pole. Labels as in (A). (**D**) Quantitative fluorescence analysis of the cell presented in (C) at different times. Labels as in (B). (**E**) FRAP analysis of FrzS-GFP fluorescence upon cellular reversal. Labels as in (A). (**F**) Quantitative fluorescence analysis of the cell presented in the (E) at different times. Labels as in (B).

were observed in 50% of the *frzCD*^{c} cells; they faded and reappeared periodically (Fig. 1C; movie S2). The cluster closer to the new brighter pole always increased in intensity before the poles switched, which suggests that these foci represent fixed sites where FrzS could accumulate transiently as it moved from pole to pole. Thus, the periodicity of FrzS oscillations is controlled by the signaling activity of the Frz pathway.

The observed FrzS oscillations could not be attributed to targeted proteolysis followed by de novo protein synthesis because chloramphenicol (Cm) did not affect reversals or FrzS pole-to-pole switching. To investigate the velocity of FrzS-GFP movements in cells, we conducted a Fluorescence Recovery After Photobleaching (FRAP) experiment in the presence of Cm. (Fig. 2, A and B). Cells expressing diffusible GFP were illuminated in a small region for 10 s, which bleached the diffusible molecules throughout the cell (Fig. 2, A and B). When moving FrzS-GFP–expressing cells were illuminated at only the dimmer cell pole for 10 s, the dimmer pole was bleached, but recovered almost full fluorescence after 40 s (Fig. 2, C and D). Thus, the movement of FrzS-GFP molecules was much slower than diffusible GFP, which suggests that it is not transported by diffusion. Moreover, fluorescence at the brighter pole was unaffected by the treatment and decreased only slightly after 40 s (Fig. 2, C and D). This suggests that the slow increase in fluorescence at the trailing pole observed before reversal (Fig. 1, B and C) was driven both by FrzS-GFP molecules that were not localized at the leading pole and FrzS-GFP molecules that came from the leading pole.

We showed that when cells reverse, the new leading pole increases in fluorescence; this increase peaked ~1 min after fluorescence dispersed at the old leading pole (Fig. 1, B and C). We used FRAP to test whether this increase was due to FrzS-GFP's leaving the old leading pole for the new leading pole. A moving cell was illuminated immediately before reversal such that only the leading pole would be unbleached. Fluorescence dispersed at the old leading pole and accumulated at the new leading pole; after 40 s most of the fluorescent signal had moved to the new leading pole (Fig. 2, E and F). Because fluorescence recovery at the new leading pole is essentially due to FrzS-GFP molecules leaving the old leading pole, we can estimate the speed of FrzS-GFP movement to be ≤ 0.3 μm/s (*12*).

In moving cells, cytosolic FrzS-GFP fluorescence could be detected as transient "comet tails" leading to the poles or as moving foci in some longer cells (see Fig. 1B; fig. S3). In many nonmoving cells, individual FrzS-GFP foci could be easily followed as they moved between cell poles (Fig. 3A; movie S3). Movement of the FrzS-GFP focus was slow: It took 5 min to travel the distance separating the two cell poles (Fig. 3A). The nonpolar fluorescence was detected as a patch, but also as a filament that overlapped the trajectory (Fig. 3B). An overlay of the time-lapse frames showed that the trajectory of the focus displayed two turns (Fig. 3B).

We also analyzed a stable mutant, *frzS*$_{\Delta 537\text{-}548}$, lacking a motif at the C-terminal end of FrzS required for polar localization (Fig. 3D). As expected, FrzS$_{\Delta 537\text{-}548}$ was unable to swarm, which indicates that polar localization is essential for function (Fig. 3C). Immunofluorescence staining of FrzS$_{\Delta 537\text{-}548}$ and deconvolution microscopy showed that FrzS organized as broad slanted bands and as clusters bordering the cell periphery (Fig. 3D). Although the pattern was not always continuous, volume reconstructions clearly showed that segments could be resolved as coiled filaments that run along the length of the cell (Fig. 3D). The localization pattern of the FrzS C-terminal variant could be due to self-organization, but it also suggests the presence of a filament that could explain the trajectory of moving FrzS-GFP foci. Indeed, FrzS$_{\Delta 537\text{-}548}$ may remain bound to the filament because it is unable either to track on the filament or to accumulate at the poles. The structures of ten FrzS$_{\Delta 537\text{-}548}$ filaments all showed turns (Fig. 3D), which suggests that these filaments could account for trajectories such as those observed (Fig. 3B).

The data presented show that S-motility reversals involve switching the sites of pili extrusion from one cell pole to the other. We hypothesize that a protein complex that contains FrzS tracks from pole to pole and controls pili assembly. Switching may be achieved by moving the complex along a cytoskeletal track (fig. S4). Bacterial cytoskeletal filaments have been shown to play an important role in the control of other cellular processes, such as cell division and DNA segregation (*13*).

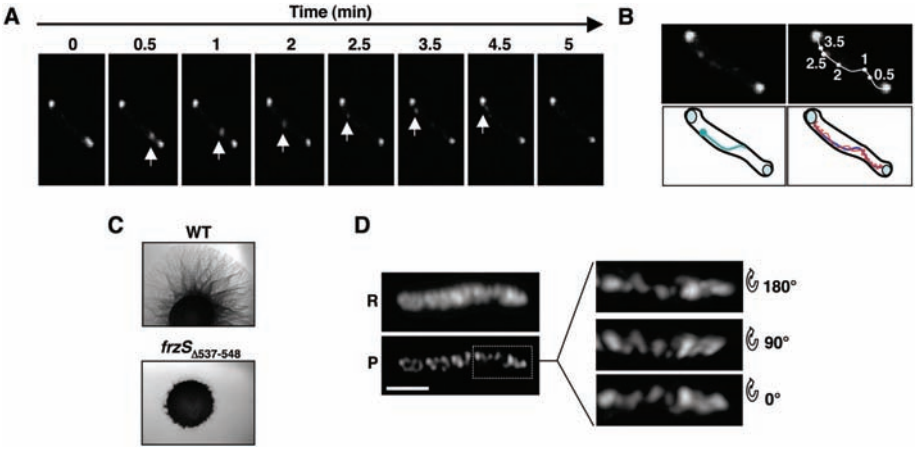

Fig. 3. FrzS may track along a helical filament. (**A**) Time-lapse fluorescence microscopy of a dynamic FrzS cluster. The cell was filmed for 5 min. White arrows point to the observed dynamic FrzS spot. (**B**) Trajectory of the moving complex. (Left) Enhanced view of the cell shown in (A) after 2.5 min (top) and schematics of the fluorescence signal (bottom). (Top right) The images shown in (A) were overlaid, and the spots observed at different times were linked to obtain a trajectory. The numbers refer to the times at which the foci were seen at a particular subcellular location. (Bottom right) Schematics of the trajectory (blue line) overlaid on the proposed coiled track (red line). (**C**) FrzS$_{\Delta 537\text{-}548}$ is defective for vegetative swarming. Motility phenotypes of the WT and *frzS*$_{\Delta 537\text{-}548}$ strains on S-motility–specific CYE-rich medium 0.3% agar plates (*11*). (**D**) Subcellular localization of FrzS$_{\Delta 537\text{-}548}$. The localization pattern of FrzS$_{\Delta 537\text{-}548}$ was determined by immunostaining using the FrzS-specific antiserum. R, raw image; P, processed image. (Right) Clockwise 90° rotations of the reconstructed volume of the segment boxed in the processed image. Scale bar, 2 μm.

References and Notes

1. J. S. Mattick, *Annu. Rev. Microbiol.* **56**, 289 (2002).
2. Y. Li *et al.*, *Proc. Natl. Acad. Sci. U.S.A.* **100**, 5443 (2003).
3. D. Bhaya, *Mol. Microbiol.* **53**, 745 (2004).
4. H. Sun, D. R. Zusman, W. Shi, *Curr. Biol.* **10**, 1143 (2000).
5. D. Kaiser, *Nat. Rev. Microbiol.* **1**, 45 (2003).
6. M. J. Ward, H. Lew, D. R. Zusman, *Mol. Microbiol.* **37**, 1357 (2000).
7. B. D. Blackhart, D. R. Zusman, *Proc. Natl. Acad. Sci. U.S.A.* **82**, 8767 (1985).
8. A. M. Spormann, D. Kaiser, *J. Bacteriol.* **181**, 2593 (1999).
9. J. M. Skerker, H. C. Berg, *Proc. Natl. Acad. Sci. U.S.A.* **98**, 6901 (2001).
10. O. A. Igoshin, A. Goldbeter, D. Kaiser, G. Oster, *Proc. Natl. Acad. Sci. U.S.A.* **101**, 15760 (2004).
11. V. H. Bustamante, I. Martinez-Flores, H. C. Vlamakis, D. R. Zusman, *Mol. Microbiol.* **53**, 1501 (2004).
12. Materials and Methods are available as supporting material on *Science* Online.
13. Z. Gitai, *Cell* **120**, 577 (2005).

14. We thank T. Alber for comments and computer analysis of FrzS. We are especially grateful to G. Oster, Y. Inclan, A. Scott, J. Viala, and K. Ryan for helpful discussions and comments on the manuscript. This research was supported by a grant from the NIH to D.R.Z. (GM20509) and an NSF graduate research fellowship to J.P.M.

Supporting Online Material

www.sciencemag.org/cgi/content/full/310/5749/855/DC1
Materials and Methods
SOM Text
Figs. S1 to S4
Table S1
Movies S1 to S3

18 August 2005; accepted 4 October 2005
10.1126/science.1119052